WAKEFIELD DAMPING IN THE DIELECTRIC ASSIST ACCELERATING STRUCTURE

Shingo Mori*, Mitsuhiro Yoshida†, KEK, Tsukuba, Japan
Daisuke Satoh‡, National Institute of Advanced Industrial Science and Technology, Tsukuba, Japan

Abstract

The dielectric-assist accelerating (DAA) structure is a dielectric-inserted normal-conducting cavity, which provides high Q value at room temperature. This cavity has the potential to apply for a long-pulse and high-duty accelerator which can provide high average current. In the high current accelerator, the wakefield from the transverse beam offset causes the emittance growth. We consider several options to dump the wakefield by modifying a radius of the beam hole and introducing a microwave absorber in the choke structure.

INTRODUCTION

A dielectric-assist accelerating (DAA) structure [1, 2] is promising in power efficiency and can be a new candidate of accelerating cavity for high duty operation because it provides high efficiency $Q \sim O(10^5)$ at room temperature and higher Q value at low temperature. Due to the structures of the dielectrics and the use of the low-loss dielectric material [2], the five cell DAA cavity provides the Q-value of 1.2×10^5 at room temperature.

In our previous work, we introduced the choke structure to the DAA cavity [3]. The motivation of this structure was to obtain better thermal contact between the copper structure and the dielectrics without brazing them inside the cavity.

Due to the high Q value of the DAA cavity, this cavity is expected to enable us the longer-pulse operation at room temperature and provide us the larger average current. However, the high-Q nature of the DAA structure would cause severe long-range wakefield. The multi-bunch instability caused by the higher-order mode or the lower-order mode would limit the maximum current from the requirement of the beam breakup, the emittance growth, and the energy spread.

Since the effect of the wakefield of the normal DAA structure has not been considered, we consider the long-range wake function by combining the analytical calculation and the numerical eigenmode simulation. Then we consider introducing the wakefield damping structure to the new design proposed in our recent work [3] and compare the long-range wake function in the normal and extended DAA structure and the C-band choke-mode cavity [4].

This paper is organized as follows. In Sec. 2, we will introduce the formulae of the longitudinal and transverse component of the long-range wake fuction and explain the eigenmode analysis we use. In Sec. 3, we will show the result of the eigenmode analysis and the obtained wake function in both normal DAA cavity and the new design. In Sec. 4, we will summarize our results.

* smori@post.kek.jp
† mitsuhiro.yoshida@kek.jp
‡ dai-satou@aist.go.jp

WAKEFUCTION CALCULATION THROUGH THE EIGENMODE ANALYSIS

We consider the equivalent circuit model of the RF cavity, where the circuit resistance corresponds to the shunt impedance of the cavity $R_z(x, y)$ in the axial direction with offset x in the x-direction and y in the y-direction. The circuit impedance for a driving frequency ω is written as

$$Z_z(x, y, \omega) = \sum_{n=0}^{\infty} \frac{R_n(x, y)}{1 + iQ_n \left(\frac{\omega}{\omega_n} - \frac{\omega_n}{\omega} \right)}, \tag{1}$$

where n is the label of all modes in the cavity without beam hole. $R_n(x, y)$ is the shunt impedance of the n-th mode. Q_n is the Q value of the n-th mode. ω_n is the eigenfrequency of the n-th mode. Since the Panofsky-Wenzel theorem relates the momentum change in the transverse direction with the transverse derivative of that in the axial direction, we can obtain

$$\frac{\omega}{c} Z_\perp(x, y, \omega) = \nabla_\perp Z_z(x, y, \omega). \tag{2}$$

Then the wake function in the axial direction and transverse direction can be obtained from the Eq. (1) as follows:

$$\begin{aligned} & w_z(x, y, s) \\ = \; & \frac{1}{2\pi} \int_{-\infty}^{\infty} d\omega Z_z(x, y, \omega) e^{i \frac{\omega s}{c}}, \\ = \; & \sum_{n=0}^{\infty} \frac{\omega_n R_n}{Q_n} \exp\left(-\frac{\omega_n s}{2Q_n c} \right) \left[\cos\left(\sqrt{1 - 1/4Q_n^2} \frac{\omega_n s}{c} \right) \right. \\ & \left. - \frac{1}{2Q_n \sqrt{1 - 1/4Q_n^2}} \sin\left(\sqrt{1 - 1/4Q_n^2} \frac{\omega_n s}{c} \right) \right], \end{aligned} \tag{3}$$

$$
\begin{aligned}
&\vec{w}_\perp(x,y,s) \\
&= \frac{i}{2\pi}\int_{-\infty}^{\infty} d\omega \vec{Z}_\perp(x,y,\omega)e^{i\frac{\omega s}{c}}, \\
&= \frac{i}{2\pi}\int_{-\infty}^{\infty} d\omega \frac{c}{\omega}\vec{\nabla}_\perp Z_z(x,y,\omega)e^{i\frac{\omega s}{c}}, \\
&= \frac{i}{2\pi}\int_{-\infty}^{\infty} d\omega \frac{c}{\omega}\sum_{n=0}^{\infty}\frac{\vec{\nabla}_\perp R_n(x,y)}{1+iQ_n\left(\frac{\omega}{\omega_n}-\frac{\omega_n}{\omega}\right)}e^{i\frac{\omega s}{c}}, \\
&= -\sum_{n=0}^{\infty}\frac{c\vec{\nabla}_\perp R_n(x,y)}{Q_n\sqrt{1-1/4Q_n^2}}\sin\left(\sqrt{1-1/4Q_n^2}\frac{\omega_n s}{c}\right) \\
&\quad \exp\left(-\frac{\omega_n s}{2Q_n c}\right). \qquad (4)
\end{aligned}
$$

Due to the dielectric structure in the DAA cavity, the eigenmodes inside the DAA structure is not a pure TM or TE modes. It is convenient to distinguish each eigenmode by using the waveform, e.g. number of nodes in the radial direction or number of the poles in the azimuthal direction in the cross-section of the transverse plane between neighboring dielectric disks.

In order to calculate the eigenmode of the DAA cavity, we calculate the unit cell of the DAA structure with one layer of the dielectric disk in the center of the unit cell and periodic boundary condition in both ends. Considering the 1 [m] accelerating cavity of the DAA structure with 37 unit cell, each eigenmode has a family of the 38 normal modes with phase advance $n\pi/37$ ($n = 0, \cdots, 37$). The normal modes of $n = 0$ are called as zero mode and those of $n = 37$ are called as π mode. The DAA structure is designed so that accelerating TM02-like mode becomes π mode.

Due to the beam-cavity interaction, the beam bunch losses energy inside the cavity and excites the eigenmodes which can decelerate the bunch. When beam has a finite offset, the deflecting modes also acquire energy from the bunch. In the family of the normal modes, the transit-time effect suppresses the non-synchronizing normal modes. Then we will consider the synchronizing normal modes for TM0m, TM1m, TE1m ($m = 1, 2$).

RESULT

Normal DAA cavity

Fig. 1 shows the schematic figure of the DAA test cavity. [2]

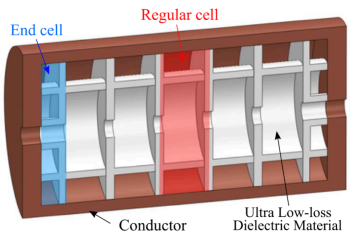

Figure 1: The normal DAA cavity of the test cavity with 6 cell.

Fig. 2 shows the dispersion curve of the normal DAA structure. Here we omit the TE0m-like modes.

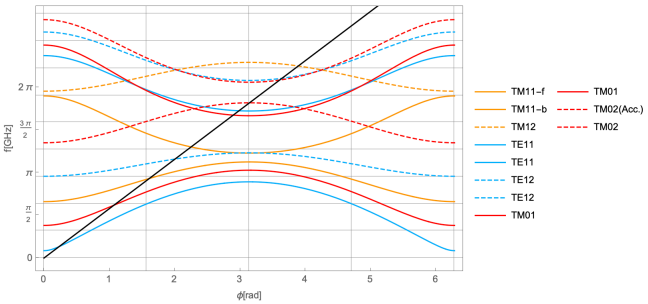

Figure 2: The dispersion curves in the normal DAA cavity. The orange curves denotes the TM1m-like mode. The blue curves denotes the TE1m-like modes. The red curve denotes the TM0m-like modes. The black line denotes the phase of the modes synchronizing with the relativistic electrons.

New design with the choke structure and the microwave absorver

In our previous work [3] we proposed to apply choke structure to the DAA structure in order to easily remove heat from the dielectric disks. Here we introduce the microwave absorber around the low-loss dielectric disks as shown in Fig. 3. The SiC ring around the dielectric disk can damp

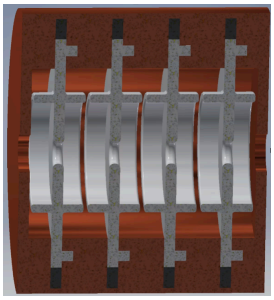

Figure 3: The new design of the DAA cavity. The white component shows the low-loss ceramics and the black component around the dielectric disk is the SiC ring as a microwave absorber.

the higher- or lower-order modes in the cavity propagating inside the transmission line. The decay length of the microwave can be estimated as

$$
d = \frac{c}{\omega}\sqrt{\frac{2}{\tan\delta(\omega)}}. \qquad (5)
$$

Fig. 4 shows the frequency dependence of the decay length of the microwave, where we use the loss tangent $\tan\delta(\omega)$ of the SiC measured by Y. Takeuchi *et al.* [5]. This curve tells us the radial thickness of SiC of 10 [mm] is enough to reduce the modes with frequency over 3 [GHz] transmitting in the radial transmission line.

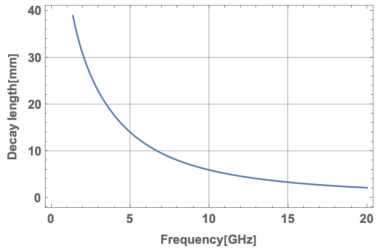

Figure 4: The frequency dependence of the decay length of the microwave in side the SiC with parameter in Ref. [5]

Fig. 5 shows the result of the longitudinal wake-function for both normal and the new DAA cavities. Since the longitudinal wake-function is dominated by the accelerating mode, the result does not change in both cavity. Fig. 6 shows the magnitude of the longitudinal wake-function at $s = 0$ for each eigenmodes in both cavity.

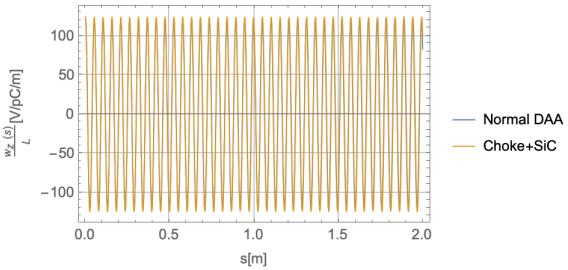

Figure 5: The longitudinal wake-function per unit length obtained from the eigenmode analysis. The blue curve denotes the result of the normal DAA cavity. The orange curve denotes the result of the new cavity.

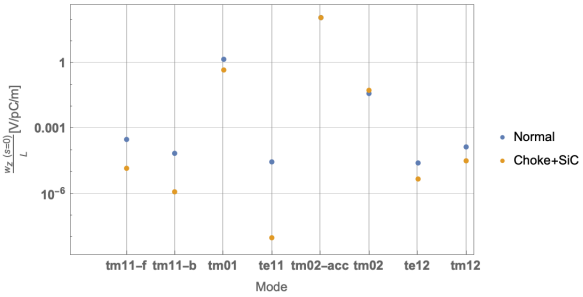

Figure 6: The contribution from each eigenmode to the longitudinal wakefunction at the origin $s = 0$.

Fig. 7 shows the result of the transverse wake function for both normal and the new DAA cavities. Here we also plot the transverse wake function obtained in the literature [4]. Fig. 8 shows the magnitude of the transverse wake-function at $s = 0.01$ [m] for each eigenmodes in both cavity.

Tab. 1 shows the frequency, the phase advance of $v_p = c$ and Q value of each eigenmodes. The frequency and the phase advance is the result of the normal DAA cavity. Note that the result of Q value does not contain the effect of the endplates, because of the models used in the eigenmode calculation have the periodic boundary.

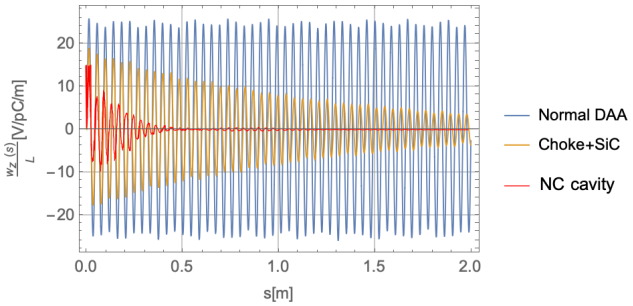

Figure 7: The transverse wake function per unit length and per unit offset calculated from the eigenmode analysis. The blue curve denotes the result of the normal DAA cavity. The orange curve denotes the result of the new DAA cavity. The red curve denotes the wake function of the normal conducting C-band structure. [4]

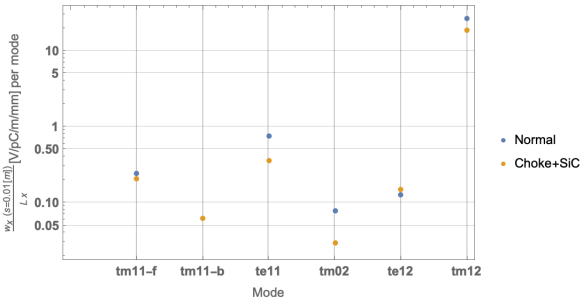

Figure 8: The contribution from each eigenmode to the transverse wakefunction at the origin $s = 0.01$ [m].

DISCUSSION AND CONCLUSION

We investigate the long-range wakefield in the DAA structure using the eigenmode analysis of both the higher order modes and the lower order modes. Since the DAA structure has about one order of magnitude higher Q value compared to the normal conducting cavity, the wakefield excited inside the DAA structure stands for a longer time than the normal conducting one. We find the wake function

mode	f [GHz]	$\frac{37\phi}{\pi}$	Q	
			Normal	Choke
TM11(+)	2.931	19	3.6×10^4	303
TM11(−)	4.093	27	1.2×10^5	1.0×10^5
TM12	7.077	−28	8.6×10^4	89
TE11	5.426	35	4.9×10^4	95
TE12	6.622	35	9.5×10^4	218
TM01	5.265	34	6.0×10^4	98
TM02Acc.	5.719	34	1.7×10^5	1.7×10^5
TM02	6.558	-32	6.2×10^4	105

Table 1: The result of the eigenmode analysis.

in the normal DAA cavity has the decay constant of 4 [μs], while the C-band choke mode cavity has the decay constant of 0.5 [ns] [4]. The new design with the choke structure and the SiC ring shown in Fig. 3 reduces the transverse wakefield well and we obtain the decay constant of 4 [ns]. Then the transverse wake effect in the new structure is improved by a thousand times better than the normal DAA structure.

This means that in the linac application for FEL the same current can be achieved by the 8 times longer flat-top length. This is promising since the high Q nature of the DAA structure can omit the pulse compressor and would provide us the longer pulse length compared with the conventional normal conducting cavity.

ACKNOWLEDGEMENTS

This work is supported by JSPS KAKENHI Grant No. 16H02134. The authors would like to thank N. Shigeoka from the Mitsubishi Heavy Industries Mechatronics Systems Ltd. for their continued support of the development of DAA structures. We thank the helpful discussion with H. Ego in KEK.

REFERENCES

[1] D Satoh, M Yoshida, and N Hayashizaki. Dielectric assist accelerating structure. *Physical Review Accelerators and Beams*, 19(1):011302, 2016.

[2] D Satoh, M Yoshida, and N Hayashizaki. Fabrication and cold test of dielectric assist accelerating structure. *Physical Review Accelerators and Beams*, 20(9):091302, 2017.

[3] Shingo Mori, Daisuke Sato, and Mitsuhiro Yoshida. The design optimization of the dielectric assist accelerating structure for better heat and gas transfer. In *10th Int. Partile Accelerator Conf.(IPAC'19), Melbourne, Australia, 19-24 May 2019*, pages 1179–1181. JACOW Publishing, Geneva, Switzerland, 2019.

[4] N Akasaka, T Shintake, and H Matsumoto. Optimization on wakefield damping in c-band accelerating structure. Technical report, SCAN-9904050, 1998.

[5] Yasunao Takeuchi, Tetsuo Abe, Tatsuya Kageyama, Hiroshi Sakai, Kazuo Yoshino, and Masahiro Ando. Control of rf dielectric properties of sic ceramics. 2010.